Transplantation of Wild-Type Hematopoietic Stem and Progenitor Cells Improves Disease Phenotypes in a Mucopolysaccharidosis IIIC Mouse Model

Rafael A. Badell-Grau[1] [iD], Kasra Pakravesh[1], Kevin Eric Thai[1], Frankie Son[1], Rola Chen[1], Joseph Rainaldi[1] [iD], Kalvin Duong[1], Pauline Losay[1], Anusha Sivakumar[1], Veenita Khare[1], Alexis N. Corl[1], Rushil Pithia[1], Christine Tran[1], Jefferey D. Esko[2], and Stephanie Cherqui[3] [iD]

Abstract

Mucopolysaccharidosis type IIIC (MPS IIIC) is a severe neurodegenerative lysosomal storage disease caused by the loss-of-function of the lysosomal transmembrane protein acetyl-CoA: heparan-α-glucosamine N-acetyltransferase. MPS IIIC is characterized by the accumulation of the glycosaminoglycan (GAG) heparan sulfate. There is no treatment for this disease. We generated a new MPS IIIC mouse model and confirmed disease phenotypes such as GAG accumulation, splenomegaly, neurological defects, and presence of disease-specific non-reducing end carbohydrates. To explore a new therapeutic strategy for this condition, we transplanted wild-type (WT) hematopoietic stem and progenitor cells (HSPCs) into lethally irradiated 2-month-old $Hgsnat^{-/-}$ mice and analyzed the resulting impact 6 months later. Transplanted HSPCs differentiated into macrophages in tissues and microglia-like cells in the brain. This resulted in a partial restoration of $Hgsnat$ expression and enzymatic activity along with a significant reduction of the MPS IIIC-specific non-reducing end carbohydrate in the treated $Hgsnat^{-/-}$ mice compared to untreated $Hgsnat^{-/-}$ mice or $Hgsnat^{-/-}$ mice transplanted with $Hgsnat^{-/-}$ HPSCs. In addition, WT HSPC transplant resulted in improved neurological defects, reduction in splenomegaly, and urine retention in the $Hgsnat^{-/-}$ mice. Furthermore, presence of glomerular hyaline bodies with focal fibrosis and sclerosis was observed in the kidney of the disease controls, whereas these abnormalities were improved in the $Hgsnat^{-/-}$ mice treated with WT HSPCs. These data support that HSPC transplantation presents a promising therapeutic avenue for MPS IIIC and represents the first step toward the clinical translation of an HSPC-mediated therapy strategy for MPS IIIC.

Keywords

lysosomal storage disorder (LSD), Sanfilippo syndrome, glycosaminoglycans (GAGs), heparan sulfate (HS), hematopoietic stem and progenitor cells (HSPCs), transmembrane lysosomal protein, macrophages, microglia

Graphical Abstract
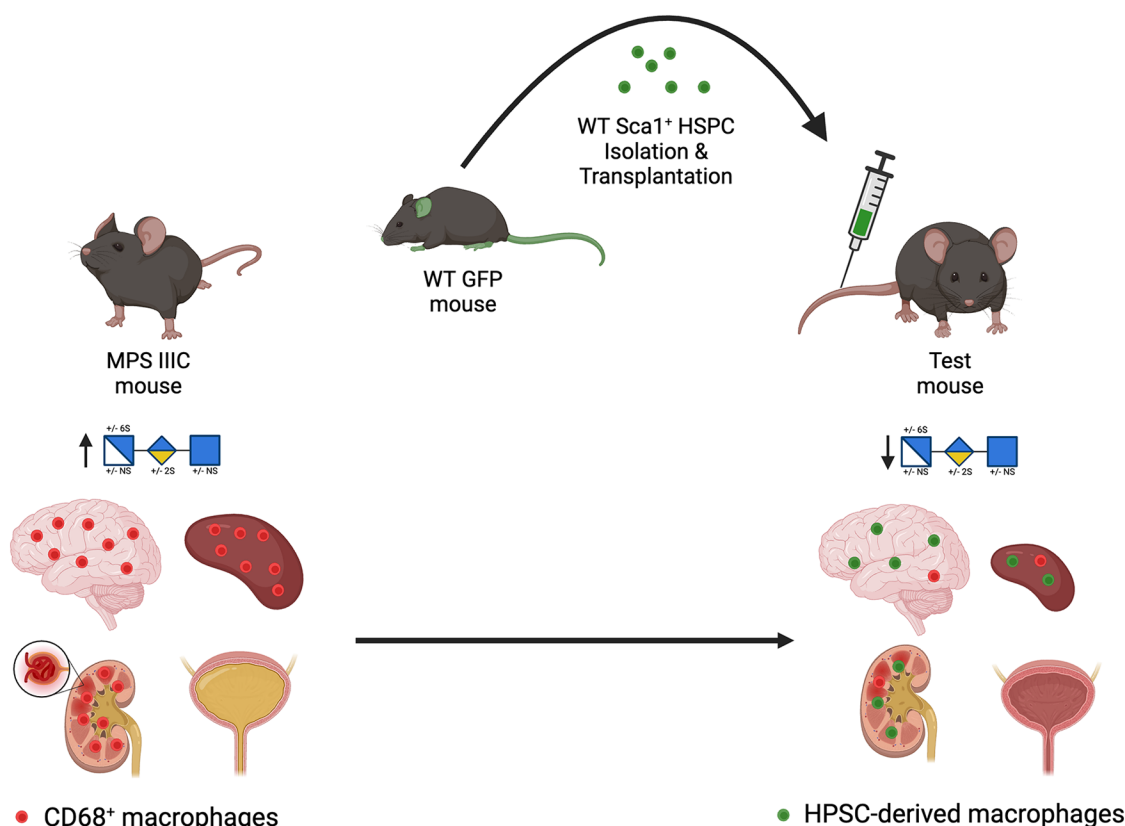
Introduction

Mucopolysaccharidosis type III (MPS III), is a group of four lysosomal storage disorders (LSDs), collectively known as Sanfilippo syndrome, characterized by intra-lysosomal accumulation of the glycosaminoglycan (GAG) heparan sulfate (HS)[1,2]. The four sub-types (types A–D) of MPS III arise from the loss of one of the four enzymes needed to breakdown HS: sulfamidase (SGSH) is affected in MPS IIIA, α-*N*-acetylglucosaminidase (NAGLU) in MPS IIIB, acetyl-CoA: heparan-α-glucosamine *N*-acetyltransferase (HGSNAT) in MPS IIIC, and *N*-acetyl glucosamine-6-sulfatase (GNS) in MPS IIID[3]. A deficiency of any of these enzymes leads to an accumulation of HS in different tissues including, the brain, spleen, and liver[4]. However, the non-reducing terminal carbohydrate structure of HS is specific to each disease sub-type[5]. These non-reducing terminal carbohydrates allow for disease-specific storage to be measured for diagnosis in patients and to assess therapeutic interventions in preclinical studies[5–8].

MPS IIIC manifests in early childhood, normally around 3 to 6 years of age. The disease normally presents with behavioral changes, developmental milestone delay, hyperactivity, organomegaly, autistic features, and motor functions, culminating in early death due to overwhelming neurodegeneration[1,3,9]. MPS IIIC has a prevalence of around 0.34 per 100,000 births[10], but recent studies have identified non-syndromic MPS IIIC patients who suffer from visual deterioration such as retinitis pigmentosa and night blindness due to loss of rod photoreceptors and severe retinal degeneration; similar ophthalmic complications are also present in the syndromic patients[11–13]. There is no effective therapy for this disease and current treatments only manage disease symptoms. For MPS IIIA, Adeno-Associated Virus

[1]Department of Pediatrics, University of California, San Diego, La Jolla, CA, USA

[2]Department of Cellular & Molecular Medicine, University of California, San Diego, La Jolla, CA, USA

[3]Division of Genetics, Department of Pediatrics, University of California, San Diego, La Jolla, CA, USA

Corresponding Author:

Stephanie Cherqui, Division of Genetics, Department of Pediatrics, University of California, 9500 Gilman Drive, MC 0734, La Jolla, CA 92093-0734, USA.
Email: scherqui@ucsd.edu

(AAV)-mediated gene therapy has been evaluated in clinical trials; one trial involved brain injections of AACrh10 over-expressing human sulfamidase (*SGSH*) which has been discontinued due to safety concerns[14], and another trial utilized intravenous administration of scAAV9-*SGSH* which resulted in a reduction in cerebrospinal fluid levels of HS as well as neurodevelopmental gain compared to natural history studies[15]. However, the HGSNAT enzyme affected in MPS IIIC is a lysosomal transmembrane enzyme, which adds complexity to the development of therapies such as adeno-associated virus gene therapy and enzyme replacement therapy[16–19].

Bone marrow transplant has been used in patients with MPS III, and the outcomes have been mixed. For MPS IIIB, some studies reported unsuccessful prevention of neurocognitive symptoms[20,21,22], and another reported possible attenuated progression of the disease in one patient[23]. In contrast, a 2.5-year-old patient affected with MPS IIIA received hematopoietic stem and progenitor cell (HSPC) transplant and showed improvement in disease phenotypes and continued cognitive development compared to six other non-treated patients with the same mutation in the *N*-sulfoglucosamine sulfohydrolase (*SGSH*) gene even 8 years later[24]. Furthermore, a recent study has shown the HSPC transplant combined with gene therapy to introduce *SGSH* under the control of a strong promoter may be effective for treating MPS IIIA as it led to decreased brain HS as well as significant improvement in neuroinflammation in MPS IIIA mice[25,26], and is now in phase I/II clinical trial in pediatric patients with promising results so far including SGSH activity detected in cerebrospinal fluid and reduction of HS storage[27]. These studies indicate that unmodified wild-type (WT) HSPC transplantation has demonstrated limited efficacy in MPS III, whereas when combined with gene therapy, HPSC transplantation enables HSPC-derived cells to overproduce the missing enzyme, leading to improved efficacy. However, MPS IIIA and MPS IIIB are caused by mutation in soluble lysosomal enzymes in contrast to MPS IIIC that is cause by mutation in a lysosomal transmembrane protein. Indeed, while cross-correction has been extensively demonstrated in several LSDs due to defective soluble lysosomal enzymes by secretion-recapture or enzyme replacement therapy, this phenomenon remains underexplored in the context of non-secreted proteins.

We previously demonstrated that transplantation of syngeneic WT HSPC could rescue cystinosis, another LSD also caused by loss of function of a lysosomal transmembrane protein, leading to long-term preservation of the kidney, eye, and thyroid structure and function[28–30]. We developed an HSPC gene therapy strategy and are currently conducting a phase I/II clinical trial for an autologous, lentiviral vector (LV)–modified, CD34$^+$ HSPC transplantation approach for cystinosis (ClinicalTrials.gov Identifier: NCT03897361). In addition, we found that a major rescue mechanism involved lysosomal cross-correction from HSPC-derived macrophages to the disease cells via tunneling nanotubes[31–33]. We have also previously demonstrated that WT HSPC transplantation led to long-term rescue in a mouse model of Friedreich's ataxia, a neurodegenerative disease, and in the 5xFAD Alzheimer's disease mice[33,34]. In both disease models, HSPCs engrafted and differentiated into microglia-like cells in the brain which led to the preservation of neurons as well as locomotor and neurological function[33,34].

In this present study, we tested the therapeutic efficacy of WT HSPC transplant in MPS IIIC. To this end, we first generated a novel mouse model of MPS IIIC, *Hgsnat*$^{–/–}$ mice, which recapitulates key features of the disease including GAG accumulation, organomegaly, and neurological deficits. Single systemic WT HSPC transplantation in *Hgsnat*$^{–/–}$ mice led to significant phenotypical benefits, representing the first step toward a clinical translation of an HSPC gene therapy strategy for MPS IIIC.

Materials and Methods

Mice

The new mouse model of MPS IIIC was generated at Jackson Laboratory by knocking out exon 2 of the *Hgsnat* gene with CRISPR/Cas9 technology with the following guide RNAs *Hgsnat*_up_crRNA1: 5′-GCGCACATGGGGTGTTGCGC-3′, *Hgsnat*_down_crRNA1: 5′-AACTCGATAGAATGTGGTCA-3′, *Hgsnat*_up_crRNA2: 5′-CTCAGAGCACGGGCGGTCTC-3′, and *Hgsnat*_down_crRNA2: 5′-AAGGATAAGAGACATCC TTA-3′. The knockout was confirmed by sequencing. Mice were bred using heterozygous breeders. Mutant mice were assigned randomly to either treated, untreated, or Mock groups, WT littermates remained as controls, and heterozygous carriers were either kept on as future breeders or sacrificed depending on the colony's needs to remain fecundity and future litters for treatment. For genotyping, tail biopsies were digested in a solution containing 200 µl of tail lyses buffer (DirectPCR, 102-T, Viagen, USA) and 3 µl of proteinase K at 55°C overnight. Samples were submitted to polymerase chain reaction (PCR) reaction with the common forward primer 5′-GTG GAC ATG GGC GAA CAA AA-3′, WT reverse primer 5′-GGG TTT CTC TGT GTA GCT CT-3′, and the mutant reverse primer 5′-TGC TGA GGA CGC GTA CAA TA-3′. Green fluorescent protein (GFP)-transgenic mice (C57B1/6-Tg (CAG-EGFP)1Osb/J; 003291, Jackson Laboratory, USA), ubiquitously expressing enhanced GFP under the control of the chicken beta-actin promoter, were used as the WT HSPC donors of HSPCs. Animals were maintained under conditions approved by the Animal Care Program (ACP) at UCSD. All procedures were approved by the Institutional Animal Care and Use Committee (IACUC). All mice were C57BL/6 background and were used at 2–10 months of age. Mice were kept in small cages provided by ACP and given continuous access to sterile food and water. Pre-established exclusion criteria were used according to IACUC guidelines and mice were assigned to treatment groups following genotyping.

HSPC Isolation, Transplantation, and Engraftment

Bone marrow cells were flushed from the femurs of 6- to 8-week-old WT, GFP-transgenic mice, one donor was usually used for two recipients. HSPCs were isolated by immunomagnetic separation using an anti-Sca1$^+$ antibody conjugated to magnetic beads (130-123-124, Miltenyi Biotec, Germany). Sca1$^+$ HSPCs were directly transplanted by tail vein injection of 2×10^6 cells resuspended in 100 µl of phosphate-buffered saline (14190-144, PBS) into lethally irradiated (7 Gy; X-Rad 320, PXi) MPS IIIC mice. Bone marrow cell engraftment of the transplanted cells was measured in peripheral blood at 8 months after transplantation. Heart puncture was performed following terminal anesthesia with ketamine (Ketaset, Zoetis), and blood was collected; 20 µl of whole blood was mixed by pipetting in 1-ml red blood cell lysis buffer (00-4333-57, eBioscience, USA) and following a 10-min incubation on ice. After incubation, 4-ml PBS were added and samples were centrifuged at $500 \times g$ for 10 min. Following centrifugation, the samples were run through a BD Accuri C6 plus flow cytometer instrument to measure GFP$^+$ cells from 10,000 live peripheral white blood cells.

Behavioral Test

Mice were tested at 10 months of age (8 months post-transplant) using two types of behavioral tests to determine gait and locomotor activity. Prior to the mice being tested, they were placed in the testing room for 30 min to acclimate to the testing environment. Open field was used to test locomotor activity using an open field arena (50×50 cm); the test was performed in the morning between 8 am and 12 pm. Mice were placed in the center of the arena and allowed to explore for 15 min while their movement was recorded using an automated tracking system (ANY-maze). Values generated by the ANY-maze software pertaining to measurable locomotor activity were collected and sorted based on treatment group to ascertain significant differences in the locomotor activity of each treatment and control group. The day after open field was done, CatWalk gait analysis was performed using an automated gait analysis system (CatWalk, Noldus Instruments, Netherlands); the test was performed in the morning between 8 am and 12 pm. Animals were placed at one end of the walkway ($130 \times 68 \times 152$ cm) and allowed to run down the length of the walkway, as two light sources illuminated the surface contact of paws with the glass floor, producing an image of a paw print. During locomotion, the glass walkway was filmed from below by a video camera. The CatWalk software program was used to analyze recorded footage, define individual paw prints, and give readouts of multiple parameters of gait. For each animal, four unbroken bouts of locomotion, during which animals ran down the walkway at a consistent speed, were used for analysis.

Urine Collection and Organomegaly

Urine volume residing in the bladder was collected using 1-ml Insulin Syringe (26027, Exel Comfort Point) and measured from terminally anesthetized mice with ketamine prior to cervical dislocation. Following sacrifice via cervical dislocation, tissues were collected from mice for downstream processing and analysis. The following tissues were collected for analysis: spleen, liver, kidney, eye, brain, and bladder. Spleen and liver masses were measured upon sacrifice and normalized to individual mouse body weight to detect organomegaly.

RNA Purification and Real-time Quantitative PCR

Tissues collected for genomic analysis were placed in 200 µl of RNAlater solution (AM7020, Invitrogen) and flash frozen in liquid nitrogen. Whole RNA extraction was performed using RNeasy Mini Kit as per manufacturer protocol (74106, Qiagen, Germany). cDNA synthesis occurred by reverse transcription (RT) of 10–15 mg tissue RNA using iScript cDNA Synthesis Kit (1708890, Bio-Rad, USA). RT-qPCR reaction assembly consisted of 10 µl iTaq Universal SYBR Green (1725121, Bio-Rad), 5 µl of 1:10 diluted cDNA (5 ng/µl), 0.4 µl forward and reverse primer (10 µM), and 4.6 µl H$_2$O, and ran on a LightCycler 480 ii (Roche, Basel, Switzerland) under the following conditions: 95°C (30 s); 40 cycles of 95°C (5 s) and 60°C (30 s); then 65°C (5 s); and 95°C (5 s). Gene expression was measured using the delta/delta CT method relative to MPS IIIC and normalized to glyceraldehyde 3-phosphate dehydrogenase (Gapdh).

HGSNAT Enzyme Activity

Enzymatic activity of the HGSNAT enzyme was assayed from flash frozen tissues extracted from mice that were not perfused as previously described[35]. Tissues were homogenized in 100 µl of MilliQ water containing protease inhibitor cocktail (P8340, Millipore Sigma, USA) using the Precellys 23 Touch Homogenizer. The total protein content of the homogenized tissue was quantified using Pierce BCA protein (23205, Thermo Fisher Scientific, USA) kit following manufacturer protocol. The samples were then made up to 10 µl in MilliQ water containing 30 µg of protein. The samples were then combined with 10 µl of McIlvain Buffer (pH 5.7) containing 3 mM of 4-methylumbelliferyl-β-D-glucosaminide (EM31025, Moscerdam), and 10 µl of 12 mM Acetyl-Coenzyme A (10101893001, Millipore Sigma) in MilliQ. Blanks with 10 µl of MilliQ water with no Acetyl-Coenzyme A were included to remove background for each sample. The reaction was incubated for 16–20 h at 37°C and stopped with the addition of 200 µl of 0.5 mM Na$_2$CO$_3$/NaHCO$_3$ (pH 10.7, S2127/S6014, Millipore Sigma) and the fluorescence measured using BioTek Synergy H1 Plate Reader.

Histopathology

Dissected tissues intended for histology staining were fixed in 10% buffered formalin (77507-018, VWR, USA) for 24 h and placed in 70% ethanol prior to being transferred to UCSD Moores Cancer Center Biorepository & Tissue Technology Center. Tissues were embedded in paraffin, sectioned at 4 µm, and stained with hematoxylin & eosin (H&E) staining to assess histological abnormalities. Kidney tissues were further analyzed to assess the degree of cortical damage and the number glomerular cells was quantified. Dr Valeria Estrada (Tissue Technology Shared Resource, Moores Cancer Center, UCSD) supervised the processing of tissues following fixation up to staining and provided a blinded histopathology report. Our team then quantified the number of normal and damaged glomeruli blindly in the whole kidney section stitched images based on the size and morphology of the glomeruli. Alcian blue staining was also performed at pH 1 in order to stain sulfated mucins such as HS.

Neurofilament Light Chain ELISA

Mice serum was collected by retro-orbital eye bleed prior to sacrifice using Micro-Hematocrit Capillary Tubes (22-362-566, Fisher Scientific, USA). Briefly, approximately 1 ml of mouse blood was collected, incubated at room temperature for 20 min, then centrifuged at $6,000 \times g$ for 15 min at 4°C, and the supernatant was collected. The serum was then stored at −80°C. Neurofilament light chain (NfL) presence in the serum was measured using the NF-L ELISA Kit (NB013370, Novus Biologicals, USA) following manufacturer's protocol and read on a VersaMax Turntable Microplate Reader (Molecular Devices, USA).

Immunofluorescence Staining, Image Acquisition, and Analysis

Tissues were fixed in 4% paraformaldehyde (J19943-K2, Thermo Fisher Scientific) for 24 h, then transferred to 10% sucrose, 20% sucrose, and 30% sucrose (S0389, Millipore Sigma) for 24 h respectively in 4°C before being embedded in Tissue-Tek Optimal Cutting Temperature buffer at −80°C (4583, Sakura Finetek, USA). Tissues then were sectioned in cryostat at a thickness of 12 µm, unmasked using citrate unmaking solution (147465, Cell Signaling Technology) through pre-warm antigen retrieval solution at 95°C for 10 min, cooled at room temperature for 15 min, and incubated in blocking solution comprised of 0.25% Triton X-100 (X100, Millipore Sigma) and 3% BSA (A3294, Millipore Sigma) in tris-buffered saline (351-086-131, Quality Biological, USA). Sections were then incubated overnight at 4°C with the following primary antibodies: chicken anti-GFP (1:200; AB290, Abcam), anti-CD68 (1:50, AB5344, Abcam), anti-IBA1 (1:500, Synaptic Systems), anti-GFAP (1:250, 50-197-5703, Fisher Scientific), and CD14 (1:250,

ab221678, Abcam, United Kingdom). The appropriate Alexa Fluor–conjugated secondary antibodies (1:1,000, A21247, PIA32728, PIA32733, A11039, Fisher Scientific) were used for the visualization of antigens. Images were captured by a Keyence microscope and Nikon Eclipse Ti2 microscope and analyzed with the ImagePro software (BitPlane, Oxford Instruments, UK). The fluorescence area was quantified from 9×9 40$\times$ stitched images per sample using Image-Pro 10 software (Media Cybernetics, USA).

Glycan Reductive Isotope Labeling Liquid Chromatography/Mass Spectrometry

Glycan Reductive Isotope Labeling Liquid Chromatography/ Mass Spectrometry (Grill LC/MS) was carried out as previously described in Lawrence et al's study[5,36]. Briefly, mouse tissues were flash frozen in liquid nitrogen and lyophilized to obtain the dry weight, based on which the concentration of the pronase in the digestion buffer was calculated. The samples were then incubated with the pronase (P5147, Millipore Sigma) on the shaker in 37°C for 24 h and subsequently in 60°C for 48 h. GAGs were eluted by loading the supernatant into Poly-Prep Chromatography columns (731-1550, Bio-Rad) filled with DEAD Sephacel beads (16550, Millipore Sigma) and then into the PD-10 desalting columns (17085101, Cytiva, USA). After the elution, GAGs were lyophilized into powder state and treated with DNase (EN0521, Thermo Fisher Scientific) and Chondroitinase ABC (C2905, Millipore Sigma) for further purification, followed by beta-elimination via incubation in NaOH overnight. The resulting solution was eluted through the two types of chromatography mentioned above again to enhance the purification, and the isolated GAGs were treated with a mixture of heparan lyases I, II, and III (50-008, 50-011, 50-012, Ibex, USA) to liberate biomarker units. After being digested with the heparan lyases, GAGs samples were spiked with standards tagged with $[^{13}C_6]$Aniline (Millipore Sigma). These were run through LC/MS using a LTQ Orbitrap Discovery electrospray ionization mass spectrometer (Thermo Scientific) equipped with quaternary high-performance liquid chromatography pump (Finnigan Surveyor MS pump) and a reverse-phase capillary column. The resulting peaks were quantified based on the known amount of the standards.

Statistical Analysis

We did not exclude any animals from our experiments. Experimenters were blinded to the genotype and treatment group of the specific sample to every extent possible. In all experiments, cohorts were age-matched. Non-objective computational measurements such as immunostaining quantification by scanning devices did not require blinding. All data are presented as the mean ± standard error of the mean (SEM), and the statistics and graphs were performed using GraphPad software Prism v.9.0. One-way analysis of variance followed
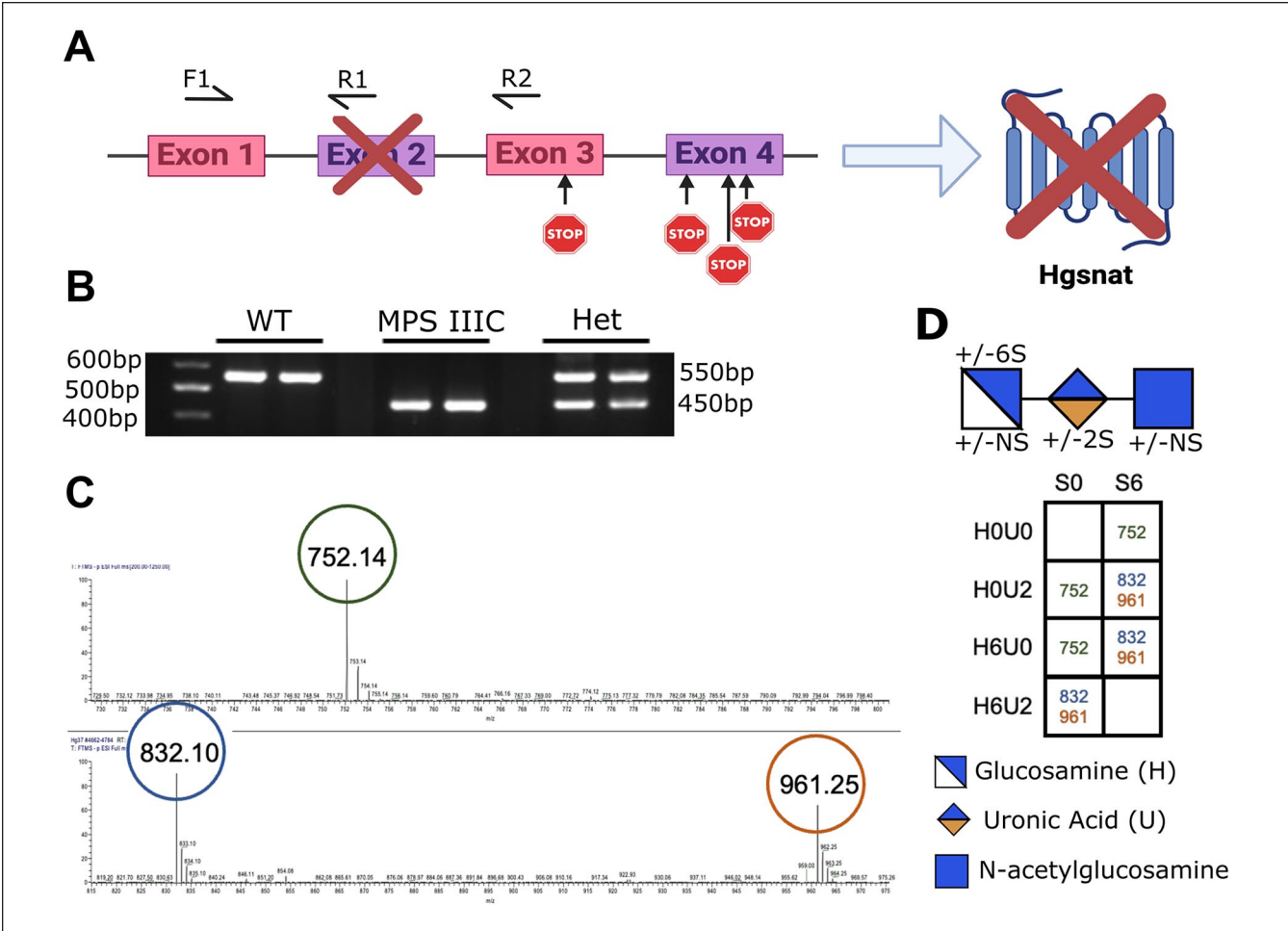
Figure 1. Generation of a novel MPS IIIC mouse model: (A) Schematic representation of the generation of a novel MPS IIIC mouse model. CRISPR/Cas9-mediated knockout of exon 2 in *Hgsnat* caused a frameshift introducing early stop codons in exons 3 and 4 leading to the absence of protein. (B) Genotyping of WT, MPS IIIC (*Hgsnat*^{−/−}), and heterozygous (*Hgsnat*+[/−]) mice was performed by PCR analysis from genomic DNA. The location of the primers is depicted in (A). F1 is a common forward primer for both WT and mutant alleles, R1 is the WT primer, and R2 is the mutant reverse primer. (C) Liquid chromatography/mass spectrometry chromatographs of $^{12}C_6$ aniline-tagged non-reducing end MPS IIIC disease-specific trisaccharide. (D) Displayed geometric symbols of the NRE carbohydrate structure and table showing the theoretically possible trisaccharide structure for MPS IIIC.

by Tukey's multiple comparisons was used to compare multiple groups unless the data were not normally distributed, where a Kruskal–Wallis followed by Dunn's multiple comparison. Statistical significance was set at $*P \leq 0.05$, $**P \leq 0.01$, $***P \leq 0.001$.

Results

Novel Mouse Model of MPS IIIC Accumulates Disease-Specific Non-reducing End Carbohydrates

To investigate the potential of WT HSPC transplantation for treating MPS IIIC, we first generated a novel MPS IIIC mouse model by removing exon 2 of the murine *Hgsnat* gene in a C57/BL6 genetic background, leading to a frameshift and early stop codons in exons 3 and 4 (Fig. 1A). This mouse model was generated due to the lack of commercially and readily available murine model of MPS IIIC. *Hgsnat* gene knockout was confirmed by sequencing (data not shown) and PCR (Fig. 1B). Curiously, breeding of heterozygote *Hgsnat* mice did not follow a Mendelian ratio, with less heterozygous mice than expected and more WT mice (chi-square = 17.974 with 2 degrees of freedom; $P = 0.0001$, $n = 608$). The quantity of knockout *Hgsnat*^{−/−} mice was as expected, and no difference in life span was observed at least up to 15 months of age (latest time point studied). We showed that the *Hgsnat*^{−/−} mice accumulate the MPS IIIC disease-specific non-reducing end carbohydrates that appear in the LC/MS at 752, 832, and 961 (Fig. 1C) with the possible structure outlined in Fig. 1D and previously reported by Lawrence and colleagues[5]. These results validate our model as MPS IIIC, and its full characterization is depicted in Fig. 1.

Transplantation of WT HSPCs Restores Partial Hgsnat *Expression and Activity in Tissues and Decreases the Disease-Specific Non-reducing End Carbohydrate in the Brain*

To assess the impact of WT HSPC transplantation on MPS IIIC, we intravenously injected lethally irradiated 6- to 8-week-old *Hgsnat*$^{-/-}$ mice with Sca1$^+$ HSPCs isolated from WT GFP-transgenic mice (Test, *n* = 12; 8 females, 4 males). As controls, we analyzed WT littermates (WT, *n* = 14; 8 females, 6 males), non-treated *Hgsnat*$^{-/-}$ mice (MPS IIIC, *n* = 11; 7 females, 4 males), and lethally irradiated *Hgsnat*$^{-/-}$ mice transplanted with Sca1$^+$ *Hgsnat*$^{-/-}$ HSPCs (Mock, *n* = 6; 2 females, 4 males). These mice were transplanted at 2 months of age and sacrificed 8 months later at 10 months of age for analysis (Fig. 2A). Donor-derived GFP$^+$ HSPC engraftment was measured in the peripheral blood of the Test mice by flow cytometry at 8 months post-transplant and ranged from 11% to 89.7% with an average of 53% engraftment (Table 1); variations in engraftment may come from tail vein injection efficiency, and differences in weight, which can affect irradiation exposure. We assessed engraftment of the WT HSPC–derived cells in tissues by measuring *Hgsnat* expression using quantitative PCR. Partial restoration of *Hgsnat* expression was observed in all the tested tissues with a recovery of *HGSNAT* expression in the Test mice compared to WT of 0.5% in the brain, 4% in the kidney, and 33% in the spleen (Fig. 2B). Similarly, presence of HGSNAT enzyme activity, as assessed by a fluorometric 4-methylubelliferone assay, was observed in tissues following WT HSPC transplantation in *Hgsnat*$^{-/-}$ mice as opposed to non-treated and Mock *Hgsnat*$^{-/-}$ mice (Fig. 2C). The level of enzyme recovery in the Test mice compared to WT was 17% in the brain, 3% in the kidney, and 27% in the spleen in which HSPC engraftment is the highest (Fig. 2C).

To evaluate the impact of WT HPSC on the pathological storage, we quantified total HS and the presence of the disease-specific non-reducing end carbohydrate in the brain and kidney by Grill LC/MS. An increase in total HS was noted in the MPS IIIC and Mock mice compared to WT controls in both tissues (Fig. 2D). A significant decrease was observed in the brains of the Test mice compared to the Mock mice, while a trend toward reduction was noted in the kidneys (Fig. 2E). Noticeably, the MPS IIIC–specific non-reducing end carbohydrate 832 was increased in both untreated and Mock groups compared to WT, and significantly decreased in the Test group compared to both non-treated *Hgsnat*$^{-/-}$ and Mock mice in both tissues (Fig. 2D, E).

Transplantation of WT HSPCs Improves Locomotor Function in the MPS IIIC Mouse Model

To assess the neurological dysfunction in the *Hgsnat*$^{-/-}$ mice, we performed behavioral testing in 10-month-old mice. We tested the locomotor activity of the mice in an open field. General motor function as expressed as mean speed and distance was significantly increased in the Test mice compared to the untreated MPS IIIC and Mock mice for mean speed, and compared to MPS IIIC group for distance (Fig. 3A). Other parameters such as time spent in the center, thigmotaxis, and freezing time did not show any significant difference between the groups (data not shown). Alterations in gait and locomotor function were demonstrated using the CatWalk testing apparatus in both the MPS IIIC and Mock groups, which displayed an inability to properly couple the movement of the right front paw with the left hind paw as well as defects in support diagonal, run average speed, duration, and run duration as compared to WT littermates (Fig. 3B and Supplemental Fig. 1). In contrast, performance of the Test mice was similar to WT mice with significantly better or non-significant trends of improvement compared to MPS IIIC and Mock mice in most of the tests (Fig. 3B). Additionally, assessment of individual paws by CatWalk gait analysis demonstrated a decrease in stride length and alterations in stance, and body speed in the MPS IIIC and Mock groups compared to the WT mice. In contrast, the Test mice behaved like WT mice with significantly better or non-significant trends of improvement compared to MPS IIIC and Mock (Fig. 3B and Supplemental Fig. 1). Altogether, these data demonstrate that MPS IIIC mice exhibit locomotor impairments caused by neurological defects, as well as potential physical abnormalities such as organomegaly and urine retention as described below. These impairments are alleviated following transplantation of WT HPSCs.

Transplantation of WT HSPC Ameliorates Urine Retention, Organomegaly, and Kidney Pathology in the MPS IIIC Mouse Model

Previous studies on MPS IIIA, B, and C have reported urine retention and distended bladder in the mouse models[4,37,38]. We confirmed the presence of urine retention and pathologically enlarged bladder in our MPS IIIC mice as well as in the Mock mice (Fig. 4A). In contrast, bladder size was decreased, and urine volume significantly reduced in the Test mice compared to MPS IIIC mice (Fig. 4B). Splenomegaly is a common feature reported in MPS III mice and patients[1,39]. Significant increase in spleen mass was observed in MPS IIIC and Mock mice compared to WT littermates while significant decrease was observed in Test mice compared to MPS IIIC and Mock mice (Fig. 4C). Hepatomegaly was also observed in the MPS III and Mock groups but was not improved in the Test group (Fig. 4D).

Brain, bladder, kidney, and spleen tissues were analyzed blindly for histopathological changes by a pathologist using H&E staining, and only the kidney exhibited marked abnormalities in the *Hgsnat*$^{-/-}$ mice. Specifically, in both untreated and Mock-treated *Hgsnat*$^{-/-}$ mice, the kidney
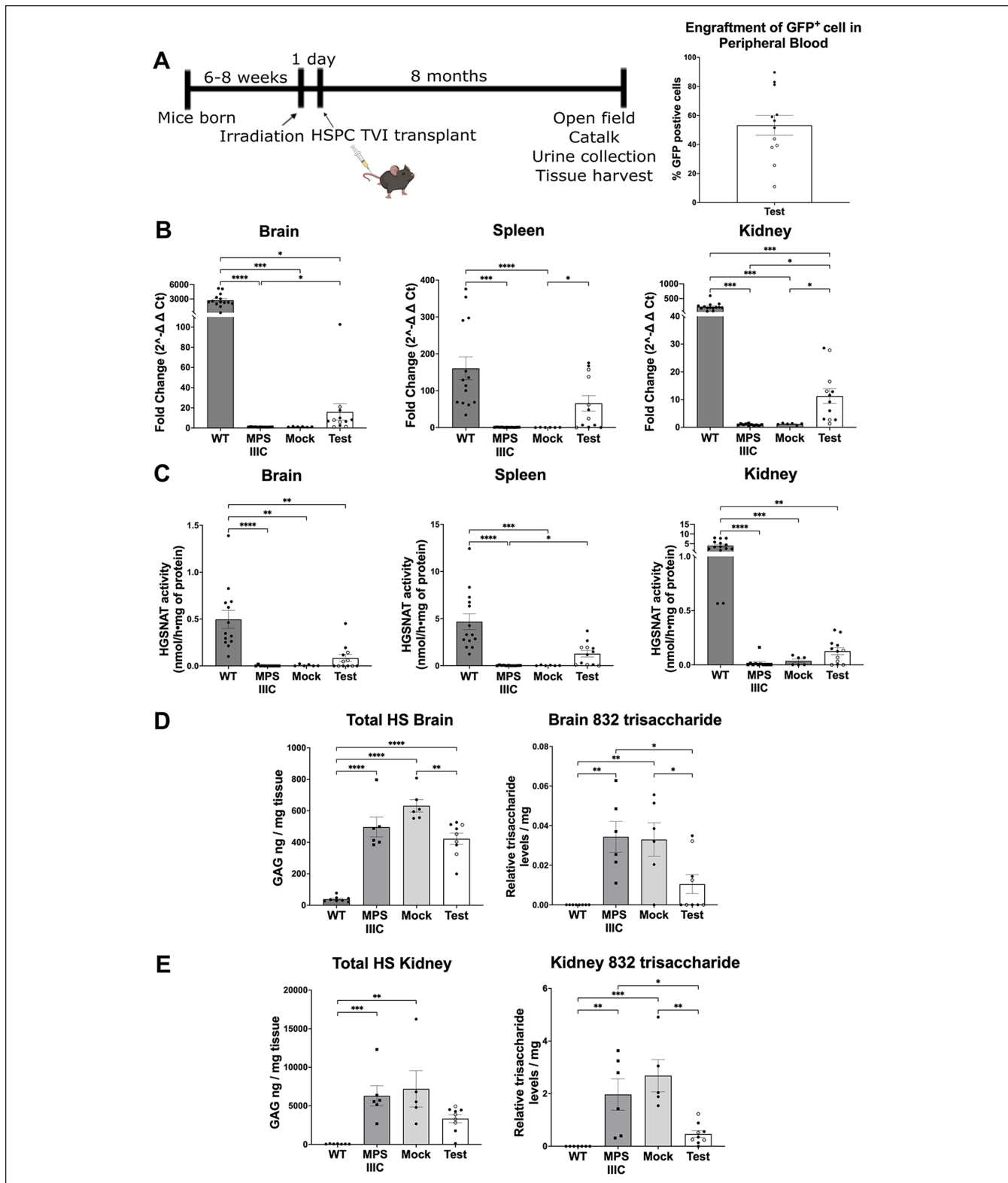
Figure 2. Transplantation of WT HSPCs leads to *Hgsnat* expression and activity in tissues. (A) Schematic representation of the experimental design and timeline. (B) *Hgsnat* mRNA expression measured by qPCR in the brain, spleen, and kidney. (C) HGSNAT enzyme activity measured using a 4-methylumbelliferone fluorescent plate assay. (D, E) LC/MS analysis of $^{12}C_6$ aniline-tagged saccharides was used to quantify total heparan sulfate (HS) in the brain and kidney. The relative levels of the MPS IIIC disease-specific non-reducing end 832 trisaccharide. For the Test mice, white dots indicate mice with peripheral blood engraftment below 50% and black dots above 50%. Data are means ± SEM. *P*-values are denoted as follows: *$P \leq 0.05$, **$P \leq 0.01$, ***$P \leq 0.001$.

Table 1. Outline of Test Mice Group Gender and Percentage HPSC Engraftment.

Mice	Gender	Engraftment of GFP+ HSPCs (% of blood)
1	Male	25.6
2	Female	38
3	Female	83
4	Male	89.7
5	Female	51.5
6	Female	60.5
7	Female	81.2
8	Female	11
9	Female	59
10	Female	56.4
11	Male	39.3
12	Male	43.9

exhibited glomerular hyaline bodies with focal fibrosis and sclerosis as well as some dilated tubules and vascular spaces (Fig. 4E). The number of damaged glomeruli was quantified and were significantly decreased compared to the MPS IIIC mice and showed non-significant trend compared to Mock mice (Fig. 4F).

To characterize the hyaline bodies in the kidney of the disease mice, we performed Alcian blue staining which is a polyvalent basic dye known to stain sulfated mucins such as HS[40]. Interestingly, Alcian blue stained primarily the glomeruli even in the WT mice (Fig. 4G), which is not surprising as HS proteoglycans are known to be a major component of the glomeruli and have an important role in glomerular organization and function[41]. Diffuse blue staining was also observed in the MPS IIIC and Mock groups, but also the presence of vacuoles, some of them containing GAGs (Fig. 4G). In contrast, the blue staining in kidney sections from Test mice was reduced, making them appear more similar to WT mice, with no visible vacuoles (Fig. 4G).

Transplantation of WT HSPC Differentiated Into Microglia-Like Cells in the Brain and Macrophages in Peripheral Tissues

We characterized the engraftment and differentiation of the GFP+ HSPCs in the brain, which were immunoreactive with Iba1 identifying these cells as microglia-like cells (Fig. 5A). We also explored tissue inflammation by examining CD68 expression which is associated with macrophages/microglia activation and phagocytic activity[42,43]. CD68 expression was significantly increased in the brain of untreated MPS IIIC and Mock mice compared to WT mice (Fig. 5B). In contrast, reduction of CD68 expression was observed in the Test mice compared to MPS IIIC and Mock mice while significance was reached compared to MPS IIIC only (Fig. 5B). In addition, neuronal damage was investigated by measuring NfL

levels in the serum[44,45]. A significant increase in NfL levels was observed in the MPS IIIC and Mock mice compared to the WT mice, which was rescued in the Test mice (Fig. 5C). Astrogliosis was also tested using anti-GFAP staining showing a non-significant increase in MPS IIIC and Mock mice, and decrease in Test mice (Supplemental Fig. 2).

We also characterized the engraftment and differentiation of GFP+ HSPCs in peripheral tissues including liver and kidney and found substantial engraftment of GFP+ HSPC–derived cells in these tissues (Fig. 5D and Supplemental Fig. 2). These cells were immunoreactive for CD14, identifying them as macrophages (Fig. 5D and Supplemental Fig. 2). Significant increase of CD14+ cells was seen only in Mock mice compared to WT probably because of the toxicity of irradiation without the positive impact of the healthy cells. In addition, significant increase of CD68-positive cells was measured in the kidney and liver from the MPS IIIC and Mock mice compared to both WT and Test mice (Fig. 5D and Supplemental Fig. 2), suggesting an increase of inflammation in the kidney and liver in the disease mice and improvement following WT HSPC transplant.

Discussion

In the present study, we explored the therapeutic potential of WT HSPC transplant for the multisystemic lysosomal storage disease MPS IIIC. MPS IIIC is caused by mutations in the *HGSNAT* gene encoding a lysosomal transmembrane enzyme. Though other MPS diseases, due to mutations in gene that encode secreted enzymes, have the potential to be treated with AAV delivery[17–19,46] or enzyme replacement therapy[47], these approaches are less effective for diseases caused by mutations in genes that encode transmembrane proteins, such as MPS IIIC[46]. Furthermore, pre-clinical studies have had limited success using AAV delivery of HGSNAT in mice models of MPS IIIC[46] and have only targeted the brain by intraparenchymal convection of AAV2-HGSNAT[48]. Another study has explored a novel rAAVhHGSNAT[EV] that contains an extracellular vesicle (EV)-mRNA-packing signal to promote HGSNAT expression and packaging into EVs, but this has only been tested *in vitro* so far[49].

Unlike AAV vectors, WT HPSCs have the ability to engraft at high level in all tissues after a single injection, as they are not restricted by dose limitations or tissue accessibility as seen in human clinical trials[50]. HSPCs then differentiate into macrophages in peripheral organs and microglia-like cells in the central nervous system (CNS) as we previously demonstrated in cystinosis, Friedreich's ataxia, and Alzheimer's disease models[29,33,34,51]. In addition, the HSPC-derived phagocytic cells can deliver healthy lysosomes carrying the transmembrane lysosomal protein to the disease cells as we demonstrated in cystinosis[31]. This process resulted in long-term tissue rescue in cystinosis[28–30], making it an appealing strategy for MPS IIIC. We confirmed in the present study the transplanted WT HSPC migration and differentiation into
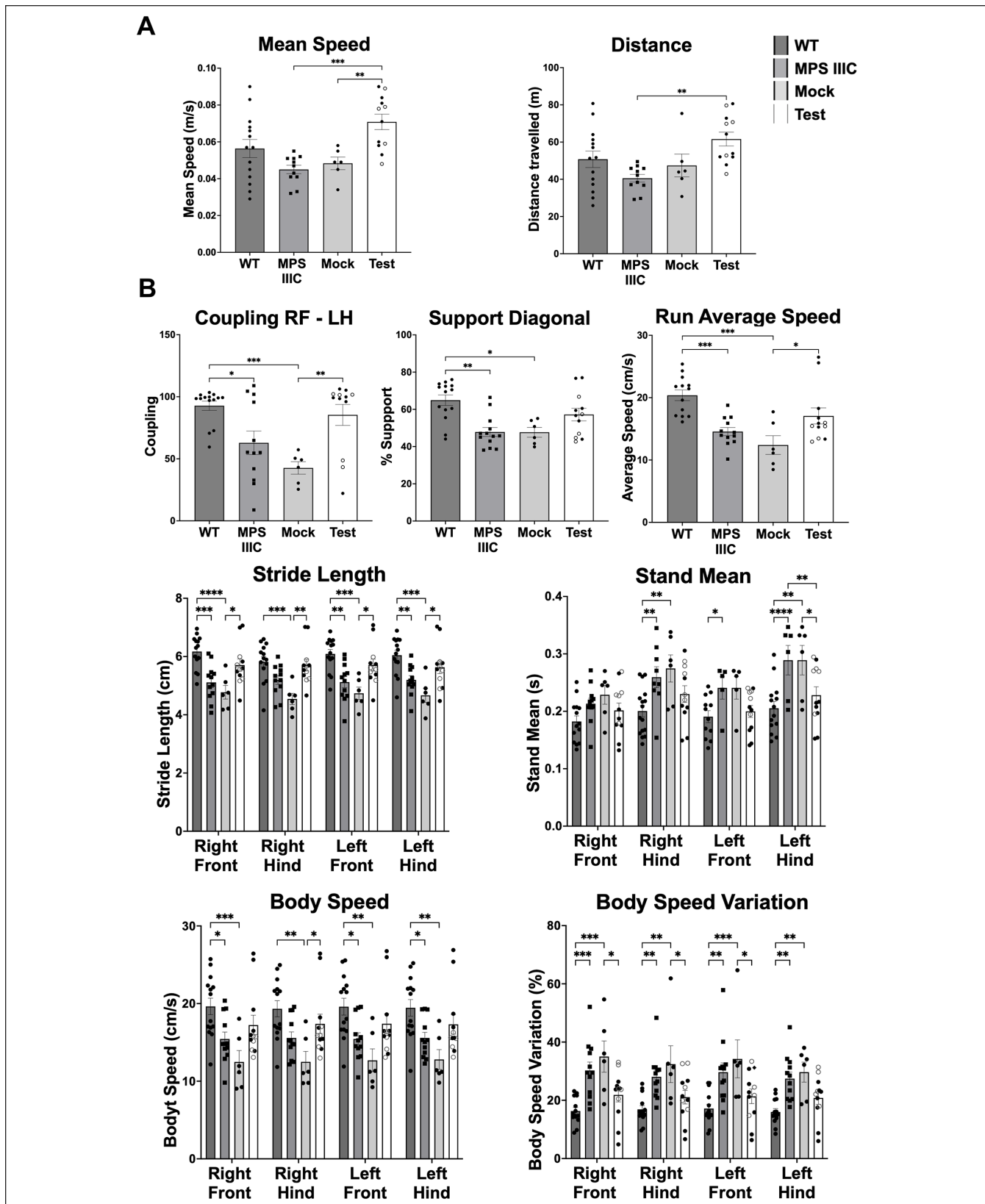
Figure 3. Transplantation of WT HSPC improves locomotor dysfunction in the *Hgsnat*$^{-/-}$ mice. (A) Open field test performed on 10-month-old mice MPS IIIC mice. (B) CatWalk gait analysis was used to assess locomotor function. For the Test mice, white dots indicate mice with peripheral blood engraftment below 50% and black dots above 50%. Data are means ± SEM. *P*-values are denoted as follows: *$P \leq 0.05$, **$P \leq 0.01$, ***$P \leq 0.001$, ****$P \leq 0.001$.
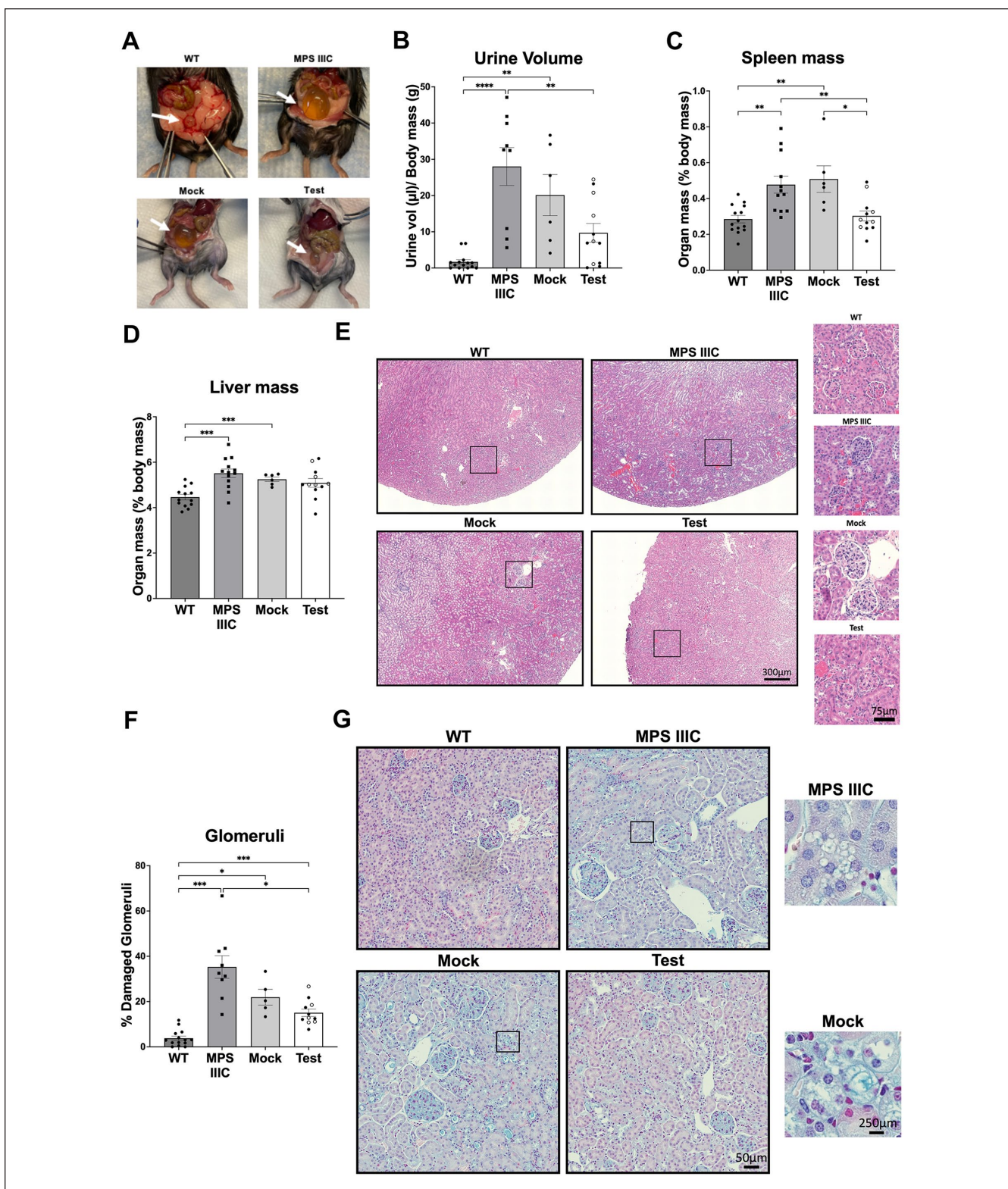
Figure 4. Transplantation of WT HSPC decreased urine retention, splenomegaly, and kidney pathology. (A) Images of mice bladders at sacrifice. (B) Urine volume as measured at sacrifice. (C) The size of the spleen was measured by weight as a percentage of body mass. (D) The size of the liver was measured by weight as a percentage of body mass. (E) Histopathology analysis of kidney sections stained by H&E. (F) Quantification of the damaged glomeruli in the different group of mice. (G) Alcian blue staining of kidney performed at pH 1 to stain-sulfated mucins include heparan sulfate. For the Test mice, white dots indicate mice with peripheral blood engraftment below 50% and black dots above 50%. Data are means ± SEM. *P*-values are denoted as follows: *$P \leq 0.05$, **$P \leq 0.01$, ***$P \leq 0.001$, ****$P \leq 0.0001$.
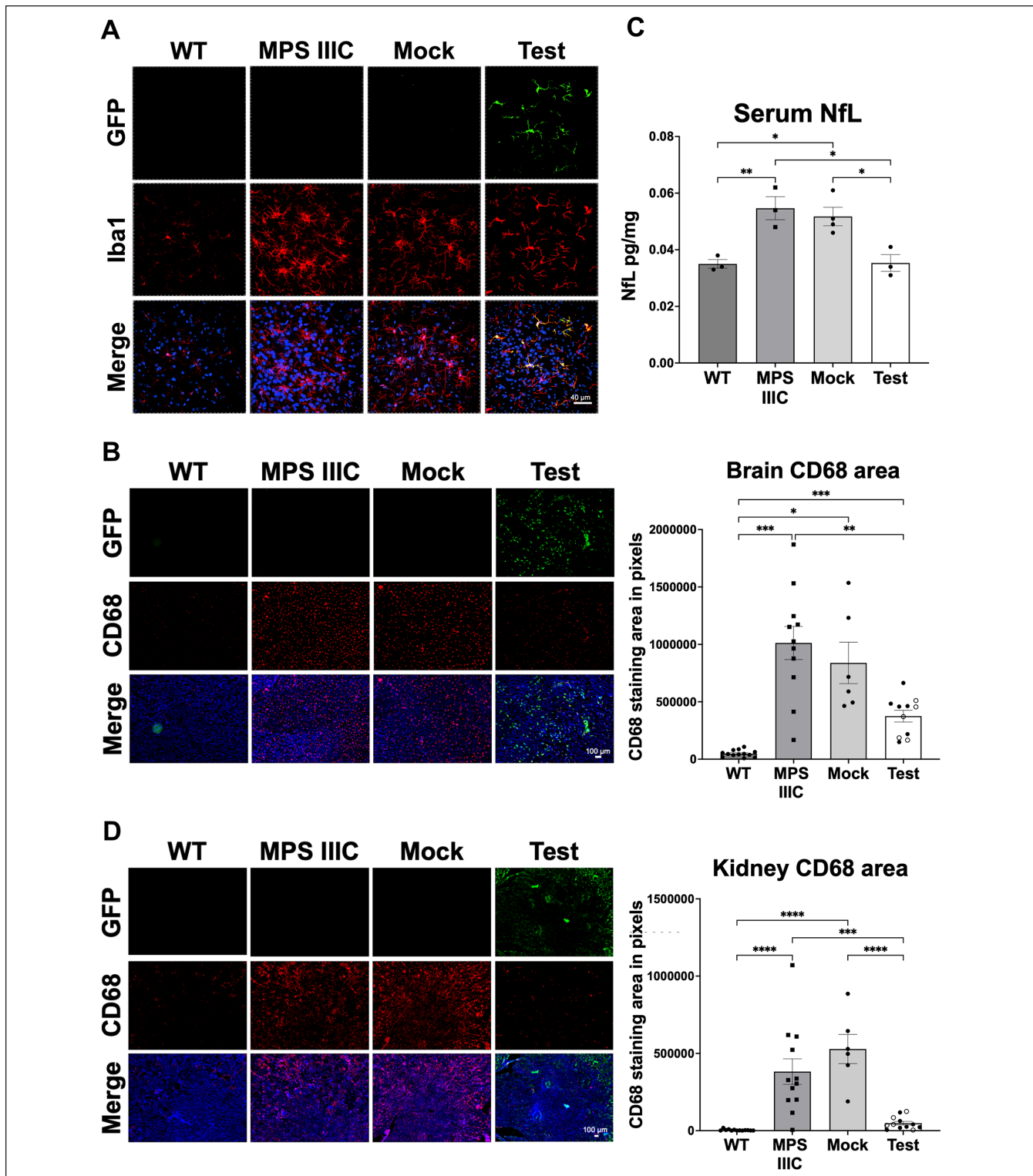
Figure 5. WT HSPC–derived cells engraft and differentiated into microglia-like cells in the brain and macrophages in tissues. (A) Representative immunofluorescence image of brain sections from WT, MPS IIIC, Mock, and Test mice stained with anti-GFP (green) and anti-Iba1 (red) antibodies. Scale bars, 40 μm. (B) Representative immunofluorescence image and area analysis quantification of brain sections from WT, MPS IIIC, Mock, and Test mice stained with anti-GFP (green) and anti-CD68 (red) antibodies. Scale bars, 100 μm. (C) NfL levels in the serum were measured by ELISA. (D) Representative immunofluorescence image and area analysis quantification of kidney sections from WT, MPS IIIC, Mock, and Test mice stained with anti-CD68 (red) antibodies. Scale bars, 100 μm. Quantification of CD68-positive staining. For the Test mice, white dots indicate mice with peripheral blood engraftment below 50% and black dots above 50%. Scale bars, 300 μm. Data are means ± SEM. *P*-values are denoted as follows: ***$P \leq 0.001$, ****$P \leq 0.0001$.

microglia-like cells in the brain and into macrophages in other peripheral tissues such as kidney in the *Hgsnat*^{−/−} mice. Another study has also shown that WT HSPC is a promising therapeutic avenue for MPS IIIC[52]. The mouse model used in this study exhibited several phenotypes similar to our model, including urine retention, hepatomegaly, splenomegaly, and increased CD68 expression in tissues. However, their model displayed hyperactivity, which we did not observe. This discrepancy may be explained by differences in the age at which behavioral assessments were performed (6 vs 10 months of age). Notably, they did not observe corrections in splenomegaly or brain HS storage, unlike our study. This discrepancy may be attributed to differences in the level of HSPC engraftment, which they did not quantify. Another possible explanation is the use of a knock-in mouse model in the Pan et al's[52] study, which expresses misfolded HGSNAT that may itself be pathogenic and limit the effectiveness of HSPC transplantation. Nonetheless, both studies support the potential of HSPC transplantation as a promising therapeutic strategy for MPS IIIC.

Representative animal models are crucial in the understanding of human diseases and for the development of novel therapies. In this study, we described a novel mouse model of MPS IIIC, which showed no activity of the HGSNAT enzyme in tissues and presented with key phenotype features of MPS IIIC disease. The hallmark of all the Sanfilippo diseases including type C is the storage of the GAG HS[1,5,39]. Using the Grill LC/MS method, we confirmed the accumulation of HS within the brain of the MPS IIIC mice as well as the presence of disease-specific non-reducing end carbohydrates[5] in the liver and brain. In addition, this new MPS IIIC model presents similar phenotype to others previously made such as splenomegaly, distended bladder, behavioral anomalies, and neuroinflammation[4,53]. Transplantation of WT HSPCs led to partial restoration of the HGSNAT enzymatic activity in the tissues and the reduction of HS and disease-specific non-reducing end carbohydrates in the brain of the *Hgsnat*^{−/−} mice, showing the positive impact of the *Hgsnat*-expressing HSPCs in MPS IIIC. It is important to note that HGSNAT enzyme activity was measured in tissues collected from mice that were not perfused, so leukocytes and other blood-derived cells could be present, potentially interfering with the enzyme activity measurement.

Patients affected with MPS IIIC develop progressive and severe neurodegenerative disease that eventually leads to loss of speech and motor function[9]. Mouse models of MPS IIIA and IIIC have shown altered locomotor activity[53,54]. We have confirmed that our mouse model of MPS IIIC also displays locomotor and neurocognitive defects such as abnormal paw coupling while walking, abnormal support diagonal, decreased stride length, and increase in body speed variation. Similar locomotor defects have been reported in another MPS IIIC mouse model[53]. Importantly, we demonstrated that a single WT HSPC transplantation led to an amelioration of these locomotor deficits. This improvement may result from the reduction of the pathological HS storage in the brain, but also from the differentiation of the WT HSPC into microglia-like cells that leads to the reduction of neuroinflammation as shown in this present study but also in MPS IIIA, IIIC, and Alzheimer's disease[26,34,52]. The improvement in locomotor defects in the *Hgsnat*^{−/−} mice following HSPC transplant could also be due to the decrease in microglia activation and inflammation in the CNS. Indeed, macrophage/microglial activation and neuroinflammation have been shown to contribute to neurodegeneration[55–57] and have been reported to present MPS IIIA[58], IIIB[58–60], and IIIC[4,53,61]. Here we showed increased expression of CD68 in the brain of the untreated and Mock-treated *Hgsnat*^{−/−} mice, which has shown to increase in microglial cells when stimulated by inflammatory cytokines[62]. In addition, significant increase of serum NfL, a marker for neuronal damage[44,45], was observed in the untreated and Mock-treated *Hgsnat*^{−/−} mice compared to WT mice. We demonstrated that both CD68 expression and NfL decreased in the *Hgsnat*^{−/−} mice treated with WT HSPC. Therefore, WT HSPC transplant therapeutic benefits in the CNS may come from the restoration of the HGSNAT in the neurons but also because of the decrease of neuroinflammation as previously shown in mouse models of MPS IIIA and IIIB[26,63].

An interesting anomaly found in other Sanfilippo mice is urine retention and distended bladder reported in the mouse models of MPS IIIA, IIIB, and IIIC[4,37,38]. We also observed an increase in urine volume and distended bladder in our *Hgsnat*^{−/−} mice as reported in another MPS IIIC mouse model[4]. The cause of urine retention is not clear and the lesion may result from infiltration of inflammatory cells throughout the entire urinary tract that could potentially lead to obstructive uropathy or disrupt the neurogenic aspect of micturition[37]. Interestingly, we showed that WT HSPC transplantation ameliorated this defect in *Hgsnat*^{−/−} mice, possibly due to the reduction of inflammatory cells into the urinary tract as observed in the kidney. Urine retention could be also due to glomerular disease[37]. Indeed, our study demonstrates the presence of kidney pathology in MPS IIIC such as glomerular hyaline bodies with focal fibrosis and sclerosis as well as some dilated tubules and vascular spaces. Similarly, a previous study showed histological alteration in the kidney in MPS IIIC mouse model[64]. HS is known to be important for glomeruli function as it is key in maintaining the selective permeability of the glomerular basement membrane[41]. Therefore, accumulation of HS may lead to morphological and functional changes in the glomeruli of the kidney. We also showed increased inflammation in the untreated and Mock-treated *Hgsnat*^{−/−} mice compared to WT mice. The histopathology defects observed in the *Hgsnat*^{−/−} kidney appeared to be improved following WT HSPC transplantation, showing direct impact of the HSPC-derived macrophages in kidney rescue. Similarly, we previously showed that WT HPSC transplantation improved kidney function,

improved structure, and decreased inflammation in the kidney in a cystinosis mouse model[65].

Our data on the impact of WT HSPCs in MPS IIIC are promising as they lead to the improvement of several complications including neurological and kidney defects as well as to the reduction of the disease-specific non-reducing end carbohydrates in the brain. However, the recovery of the expression of *Hgsnat* and its enzyme activity was limited in tissues. HPSC transplant has been explored for other MPS diseases and while MPS I can be rescued by WT HSPC transplantation, bone marrow transplantation was not always able to significantly improve or stabilize cognitive function in MPS IIIA patients[21]. Similarly, bone marrow transplant in MPS IIIA murine neonates did not reduce HS storage in the brain, but the donor cell engraftment was low (~20%)[66]. The hypothesis for these results was that *SGSH* was not sufficiently expressed in HSPC-derived macrophages/microglia in tissues. Further studies support this hypothesis as MPS IIIA adult mice showed that both WT HSPC and LV-transduced MPS IIIA HSPCs, with SGSH expression driven under a spleen focus-forming virus promoter, were effective at reducing GM2 gangliosides and neuroinflammation[26], but not in reducing HS or improving behavior[26]. In contrast, LV-SGSH-transduced HSPCs that led to ubiquitous over-expression (phosphoglycerate kinase promoter) resulted in normalization of HS, and significant reduction in neuroinflammation and improvement of behavior[26,67]. Similarly, the same group showed that MPS IIIA HSPCs transduced with a LV-SGSH, carrying the myeloid-specific promoter CD11b, were successful in rescuing brain HS, GM2 gangliosides, and neuroinflammation[67]. A clinical trial is now ongoing for MPS IIIA using this approach with promising clinical outcome (ClinicalTrials.gov Identifier: NCT04201405). We believe that similar to MPS IIIA, the HGSNAT enzyme is not well expressed in HSPC-derived cells leading to a significant impact of the WT HSPCs, and HSPC gene therapy should lead to even greater therapeutic beneficial the outcomes.

Our findings demonstrate WT HSPC transplantation led to the improvement of disease phenotypes including locomotor defects, urine retention, kidney pathology, splenomegaly, as well as a reduction in disease-specific non-reducing end carbohydrate despite recovery of HGSNAT enzyme activity in tissues. Therefore, these results are promising and support the development of an autologous transplantation of gene-modified HSPCs to drive a strong and ubiquitous expression of *HGSNAT*.

Acknowledgments

ORCID iDs

Rafael A. Badell-Grau (iD) https://orcid.org/0000-0001-7640-822X
Joseph Rainaldi (iD) https://orcid.org/0000-0003-4123-0008
Stephanie Cherqui (iD) https://orcid.org/0000-0003-1240-5219

Statements and Declarations

Ethical Approval

This study was approved by our institutional review board.

Funding

Declaration of Conflicting Interests

The author(s) declared the following potential conflicts of interest with respect to the research, authorship, and/or publication of this article: Stephanie Cherqui is a cofounder, shareholder, and a member of both the Scientific Board and board of directors of Papillon Therapeutics Inc Stephanie Cherqui is also of the Chair of the Scientific Review Board and a member of Board of Trustees of the Cystinosis Research Foundation. This work is covered in the patent entitled "Methods of Treating Lysosomal Disorders" (#US-2024-0009247-A1). Anusha Sivakumar is a consultant for Papillon Therapeutics, Inc and receives income. The terms of these arrangement have been reviewed and approved by the University of California San Diego in accordance with its conflict-of-interest policies.

Statement of Human and Animal Rights

This article does not contain any studies with human The Univesity of California, San Diego AInstitutional Animal Care and Use Committee approved the experiemental procedures used in this study (approval S12288.) on June 17, 2021.

Statement of Informed Consent

There are no human subjects in this article and informed consent is not applicable.

Data Availability Statement

All relevant data included in the paper are available from the corresponding author upon reasonable request.

Supplemental Material

Supplemental material for this article is available online.

References

1. Ruijter GJ, Valstar MJ, van de Kamp JM, van der Helm RM, Durand S, van Diggelen OP, Wevers RA, Poorthuis BJ, Pshezhetsky AV, Wijburg FA. Clinical and genetic spectrum of Sanfilippo type C (MPS IIIC) disease in The Netherlands. *Mol Genet Metab*. 2008;93(2):104–11. doi:10.1016/j.ymgme.2007.09.011.

2. Pollock K, Noritake S, Imai DM, Pastenkos G, Olson M, Cary W, Yang S, Fierro FA, White J, Graham J, Dahlenburg H, et al. An immune deficient mouse model for mucopolysaccharidosis IIIA (Sanfilippo syndrome). *Sci Rep*. 2023;13(1):18439. doi:10.1038/s41598-023-45178-0.

3. Héron B, Mikaeloff Y, Froissart R, Caridade G, Maire I, Caillaud C, Levade T, Chabrol B, Feillet F, Ogier H, Valayannopoulos V, et al. Incidence and natural history of mucopolysaccharidosis type III in France and comparison with United Kingdom and Greece. *Am J Med Genet A*. 2011;155A(1):58–68. doi:10.1002/ajmg.a.33779.

4. Martins C, Hůlková H, Dridi L, Dormoy-Raclet V, Grigoryeva L, Choi Y, Langford-Smith A, Wilkinson FL, Ohmi K, DiCristo G, Hamel E, et al. Neuroinflammation, mitochondrial defects and neurodegeneration in mucopolysaccharidosis III type C mouse model. *Brain*. 2015;138(pt 2):336–55. doi:10.1093/brain/awu355.

5. Lawrence R, Brown JR, Al-Mafraji K, Lamanna WC, Beitel JR, Boons GJ, Esko JD, Crawford BE. Disease-specific non-reducing end carbohydrate biomarkers for mucopolysaccharidoses. *Nat Chem Biol*. 2012;8(2):197–204. doi:10.1038/nchembio.766.

6. Kan SH, Aoyagi-Scharber M, Le SQ, Vincelette J, Ohmi K, Bullens S, Wendt DJ, Christianson TM, Tiger PMN, Brown JR, Lawrence R, et al. Delivery of an enzyme-IGFII fusion protein to the mouse brain is therapeutic for mucopolysaccharidosis type IIIB. *Proc Natl Acad Sci USA*. 2014;111(41):14870–75. doi:10.1073/pnas.1416660111.

7. Lawrence R, Brown JR, Lorey F, Dickson PI, Crawford BE, Esko JD. Glycan-based biomarkers for mucopolysaccharidoses. *Mol Genet Metab*. 2014;111(2):73–83. doi:10.1016/j.ymgme.2013.07.016.

8. Magat J, Jones S, Baridon B, Agrawal V, Wong H, Giaramita A, Mangini L, Handyside B, Vitelli C, Parker M, Yeung N, et al. Intracerebroventricular dosing of N-sulfoglucosamine sulfohydrolase in mucopolysaccharidosis IIIA mice reduces markers of brain lysosomal dysfunction. *J Biol Chem*. 2022;298(12):102625. doi:10.1016/j.jbc.2022.102625.

9. Delgadillo V, O'Callaghan M, del Gort L, Coll M, Pineda M. Natural history of Sanfilippo syndrome in Spain. *Orphanet J Rare Dis*. 2013;8(1):189. doi:10.1186/1750-1172-8-189.

10. Hult M, Darin N, von Döbeln U, Månsson JE. Epidemiology of lysosomal storage diseases in Sweden. *Acta Paediatr*. 2014;103(12):1258–63. doi:10.1111/apa.12807.

11. Ludwig J, Sawant OB, Wood J, Singamsetty S, Pan X, Bonilha VL, Rao S, Pshezhetsky AV. Histological characterization of retinal degeneration in mucopolysaccharidosis type IIIC. *Exp Eye Res*. 2023;229:109433. doi:10.1016/j.exer.2023.109433.

12. Haer-Wigman L, Newman H, Leibu R, Bax NM, Baris HN, Rizel L, Banin E, Massarweh A, Roosing S, Lefeber DJ, Zonneveld-Vrieling MN, et al. Non-syndromic retinitis pigmentosa due to mutations in the mucopolysaccharidosis type IIIC gene, heparan-alpha-glucosaminide N-acetyltransferase (HGSNAT). *Hum Mol Genet*. 2015;24:3742–51. doi:10.1093/hmg/ddv118.

13. Canals I, Soriano J, Orlandi JG, Torrent R, Richaud-Patin Y, Jiménez-Delgado S, Merlin S, Follenzi A, Consiglio A, Vilageliu L, Grinberg D, et al. Activity and high-order effective connectivity alterations in Sanfilippo C patient-specific neuronal networks. *Stem Cell Reports*. 2015;5(4):546–57. doi:10.1016/j.stemcr.2015.08.016.

14. Bugiani M, Abbink TEM, Edridge AWD, van der Hoek L, Hillen AEJ, van Til NP, Hu-A-Ng GV, Breur M, Aiach K, Drevot P, Hocquemiller M, et al. Focal lesions following intracerebral gene therapy for mucopolysaccharidosis IIIA. *Ann Clin Transl Neurol*. 2023;10(6):904–17. doi:10.1002/acn3.51772.

15. Flanigan KM, Smith N, Couce ML, Rajan D, Truxal K, McBride KL, De Castro Lopez MJ, Fuller M, Taylor J, Del Campo AB, Grachev I, et al. Interim results of Transpher A, a multicenter, single-dose clinical trial of UX111 gene therapy for Sanfilippo syndrome type A (mucopolysaccharidosis IIIA). *Mol Genet Metab*. 2023;138(2):107101. doi:10.1016/j.ymgme.2022.107101.

16. Hughes MP, Smith DA, Morris L, Fletcher C, Colaco A, Huebecker M, Tordo J, Palomar N, Massaro G, Henckaerts E, Waddington SN, et al. AAV9 intracerebroventricular gene therapy improves lifespan, locomotor function and pathology in a mouse model of Niemann–Pick type C1 disease. *Hum Mol Genet*. 2018;27(17):3079–98. doi:10.1093/hmg/ddy212.

17. Duncan FJ, Naughton BJ, Zaraspe K, Murrey DA, Meadows AS, Clark KR, Newsom DE, White P, Fu H, McCarty DM. Broad functional correction of molecular impairments by systemic delivery of scAAVrh74-hSGSH gene delivery in MPS IIIA mice. *Mol Ther*. 2015;23(4):638–47. doi:10.1038/mt.2015.9.

18. Heldermon CD, Qin EY, Ohlemiller KK, Herzog ED, Brown JR, Vogler C, Hou W, Orrock JL, Crawford BE, Sands MS. Disease correction by combined neonatal intracranial AAV and systemic lentiviral gene therapy in Sanfilippo syndrome type B mice. *Gene Ther*. 2013;20(9):913–21. doi:10.1038/gt.2013.14.

19. Roca C, Motas S, Marcó S, Ribera A, Sánchez V, Sánchez X, Bertolin J, León X, Pérez J, Garcia M, Villacampa P, et al. Disease correction by AAV-mediated gene therapy in a new mouse model of mucopolysaccharidosis type IIID. *Hum Mol Genet*. 2017;26(8):1535–51. doi:10.1093/hmg/ddx058.

20. Vellodi A, Young E, New M, Pot-Mees C, Hugh-Jones K. Bone marrow transplantation for Sanfilippo disease type B. *J Inherit Metab Dis*. 1992;15(6):911–18. doi:10.1007/BF01800232.

21. Sivakumur P, Wraith JE. Bone marrow transplantation in mucopolysaccharidosis type IIIA: a comparison of an early treated patient with his untreated sibling. *J Inherit Metab Dis*. 1999;22(7):849–50. doi:10.1023/A:1005526628598.

22. Taylor M, Khan S, Stapleton M, Wang J, Chen J, Wynn R, Yabe H, Chinen Y, Boelens JJ, Mason RW, Kubaski F, et al. Hematopoietic stem cell transplantation for mucopolysaccharidoses: past, present, and future. *Biol Blood*

Marrow Transplant. 2019;25(7):e226–46. doi:10.1016/j.bbmt.2019.02.012.

23. Shimada T, Kelly J, LaMarr WA, van Vlies N, Yasuda E, Mason RW, Mackenzie W, Kubaski F, Giugliani R, Chinen Y, Yamaguchi S, et al. Novel heparan sulfate assay by using automated high-throughput mass spectrometry: application to monitoring and screening for mucopolysaccharidoses. *Mol Genet Metab*. 2014;113(1–2):92–99. doi:10.1016/j.ymgme.2014.07.008.

24. Köhn AF, Grigull L, du Moulin M, Kabisch S, Ammer L, Rudolph C, Muschol NM. Hematopoietic stem cell transplantation in mucopolysaccharidosis type IIIA: a case description and comparison with a genotype-matched control group. *Mol Genet Metab Rep*. 2020;23:100578. doi:10.1016/j.ymgmr.2020.100578.

25. Ellison SM, Liao A, Wood S, Taylor J, Youshani AS, Rowlston S, Parker H, Armant M, Biffi A, Chan L, Farzaneh F, et al. Pre-clinical safety and efficacy of lentiviral vector-mediated ex vivo stem cell gene therapy for the treatment of mucopolysaccharidosis IIIA. *Mol Ther Methods Clin Dev*. 2019;13:399–413. doi:10.1016/j.omtm.2019.04.001.

26. Langford-Smith A, Wilkinson FL, Langford-Smith KJ, Holley RJ, Sergijenko A, Howe SJ, Bennett WR, Jones SA, Wraith J, Merry CL, Wynn RF, et al. Hematopoietic stem cell and gene therapy corrects primary neuropathology and behavior in mucopolysaccharidosis IIIA mice. *Mol Ther*. 2012;20(8):1610–21. doi:10.1038/mt.2012.82.

27. Jones S, Kinsella J, Holley RJ, Potter J, Booth C, Buckland K, Rust S, Bromley R, Church HJ, Lee H, Ford L, et al. Clinical outcomes and sustained biochemical engraftment following ex-vivo autologous stem cell gene therapy for mucopolysaccharidosis type IIIA. *Mol Genet Metab*. 2024;141(2):107905. doi:10.1016/j.ymgme.2023.107905.

28. Gaide Chevronnay HP, Janssens V, Van Der Smissen P, Rocca CJ, Liao XH, Refetoff S, Pierreux CE, Cherqui S, Courtoy PJ. Hematopoietic stem cells transplantation can normalize thyroid function in a cystinosis mouse model. *Endocrinology*. 2016;157(4):1363–71. doi:10.1210/en.2015-1762.

29. Harrison F, Yeagy BA, Rocca CJ, Kohn DB, Salomon DR, Cherqui S. Hematopoietic stem cell gene therapy for the multisystemic lysosomal storage disorder cystinosis. *Mol Ther*. 2013;21(2):433–44. doi:10.1038/mt.2012.214.

30. Syres K, Harrison F, Tadlock M, Jester JV, Simpson J, Roy S, Salomon DR, Cherqui S. Successful treatment of the murine model of cystinosis using bone marrow cell transplantation. *Blood*. 2009;114(12):2542–52. doi:10.1182/blood-2009-03-213934.

31. Naphade S, Sharma J, Gaide Chevronnay HP, Shook MA, Yeagy BA, Rocca CJ, Ur SN, Lau AJ, Courtoy PJ, Cherqui S. Brief reports: lysosomal cross-correction by hematopoietic stem cell-derived macrophages via tunneling nanotubes. *Stem Cells*. 2015;33(1):301–309. doi:10.1002/stem.1835.

32. Goodman S, Naphade S, Khan M, Sharma J, Cherqui S. Macrophage polarization impacts tunneling nanotube formation and intercellular organelle trafficking. *Sci Rep*. 2019;9(1):14529. doi:10.1038/s41598-019-50971-x.

33. Rocca CJ, Goodman SM, Dulin JN, Haquang JH, Gertsman I, Blondelle J, Smith JLM, Heyser CJ, Cherqui S. Transplantation of wild-type mouse hematopoietic stem and progenitor cells ameliorates deficits in a mouse model of Friedreich's ataxia. *Sci Transl Med*. 2017;9(413):eaaj2347. doi:10.1126/scitranslmed.aaj2347.

34. Mishra P, Silva A, Sharma J, Nguyen J, Pizzo D, Sahoo D, Cherqui S. Transplantation of wild-type hematopoietic stem and progenitor cells rescue Alzheimer's disease in a mouse model and highlights the central role of microglia in disease pathogenesis. 2022. doi:10.21203/rs.3.rs-1602615/v1.

35. Voznyi YaV, Karpova EA, Dudukina TV, Tsvetkova IV, Boer AM, Janse HC, van Diggelen OP. A fluorimetric enzyme assay for the diagnosis of Sanfilippo disease C (MPS III C). *J Inherit Metab Dis*. 1993;16(2):465–72. doi:10.1007/BF00710299.

36. Lawrence R, Olson SK, Steele RE, Wang L, Warrior R, Cummings RD, Esko JD. Evolutionary differences in glycosaminoglycan fine structure detected by quantitative glycan reductive isotope labeling. *J Biol Chem*. 2008;283(48):33674–84. doi:10.1074/jbc.M804288200.

37. Gografe SI, Sanberg PR, Chamizo W, Monforte H, Garbuzova-Davis S. Novel pathologic findings associated with urinary retention in a mouse model of mucopolysaccharidosis type IIIB. *Comp Med*. 2009;59(3):139–46.

38. Langford-Smith A, Langford-Smith KJ, Jones SA, Wynn RF, Wraith JE, Wilkinson FL, Bigger BW. Female mucopolysaccharidosis IIIA mice exhibit hyperactivity and a reduced sense of danger in the open field test. *PLoS ONE*. 2011;6(10):e25717. doi:10.1371/journal.pone.0025717.

39. Wijburg FA, Węgrzyn G, Burton BK, Tylki-Szymańska A. Mucopolysaccharidosis type III (Sanfilippo syndrome) and misdiagnosis of idiopathic developmental delay, attention deficit/hyperactivity disorder or autism spectrum disorder. *Acta Paediatrica*. 2013;102(5):462–70. doi:10.1111/apa.12169.

40. Padra JT, Lindén SK. Optimization of Alcian blue pH 1.0 histo-staining protocols to match mass spectrometric quantification of sulfomucins and circumvent false positive results due to sialomucins. *Glycobiology*. 2022;32(1):6–10. doi:10.1093/glycob/cwab091.

41. Heintz B, Stöcker G, Mrowka C, Rentz U, Melzer H, Stickeler E, Sieberth HG, Greiling H, Haubeck HD. Decreased glomerular basement membrane heparan sulfate proteoglycan in essential hypertension. *Hypertension*. 1995;25(3):399–407. doi:10.1161/01.HYP.25.3.399.

42. Hopperton KE, Mohammad D, Trépanier MO, Giuliano V, Bazinet RP. Markers of microglia in post-mortem brain samples from patients with Alzheimer's disease: a systematic review. *Mol Psychiatry*. 2018;23(2):177–98. doi:10.1038/mp.2017.246.

43. Lier J, Streit WJ, Bechmann I. Beyond activation: characterizing microglial functional phenotypes. *Cells*. 2021;10(9):2236. doi:10.3390/cells10092236.

44. Bhalla A, Ravi R, Fang M, Arguello A, Davis SS, Chiu CL, Blumenfeld JR, Nguyen HN, Earr TK, Wang J, Astarita G, et al. Characterization of fluid biomarkers reveals lysosome dysfunction and neurodegeneration in neuronopathic MPS II patients. *IJMS*. 2020;21(15):5188. doi:10.3390/ijms21155188.

45. Winner LK, Rogers ML, Snel MF, Hemsley KM. Biomarkers for predicting disease course in Sanfilippo syndrome: an urgent unmet need in childhood-onset dementia. *J Neurochem*. 2023;166(3):481–96. doi:10.1111/jnc.15891.

46. Tordo J, O'Leary C, Antunes ASLM, Palomar N, Aldrin-Kirk P, Basche M, Bennett A, D'Souza Z, Gleitz H, Godwin A,

Holley RJ, et al. A novel adeno-associated virus capsid with enhanced neurotropism corrects a lysosomal transmembrane enzyme deficiency. *Brain*. 2018;141(7):2014–31. doi:10.1093/brain/awy126.

47. Rohrbach M, Clarke JT. Treatment of lysosomal storage disorders: progress with enzyme replacement therapy. *Drugs*. 2007;67(18):2697–716. doi:10.2165/00003495-200767180-00005.

48. O'Leary C, Forte G, Mitchell NL, Youshani AS, Dyer A, Wellby MP, Russell KN, Murray SJ, Jolinon N, Jones SA, Stacey K, et al. Intraparenchymal convection enhanced delivery of AAV in sheep to treat mucopolysaccharidosis IIIC. *J Transl Med*. 2023;21(1):437. doi:10.1186/s12967-023-04208-1.

49. Bobo TA, Robinson M, Tofade C, Sokolski-Papkov M, Nichols P, Vorobiov S, Fu H. AAV gene replacement therapy for treating MPS IIIC: facilitating bystander effects via EV-mRNA cargo. *J Extracell Vesicles*. 2024;13(7):e12464. doi:10.1002/jev2.12464.

50. Ertl HCJ. Immunogenicity and toxicity of AAV gene therapy. *Front Immunol*. 2022;13:975803. doi:10.3389/fimmu.2022.975803.

51. Cherqui S. Hematopoietic stem cell gene therapy for cystinosis: from bench-to-bedside. *Cells*. 2021;10(12):3273. doi:10.3390/cells10123273.

52. Pan X, Caillon A, Fan S, Khan S, Tomatsu S, Pshezhetsky AV. Heterologous HSPC transplantation rescues neuroinflammation and ameliorates peripheral manifestations in the mouse model of lysosomal transmembrane enzyme deficiency, MPS IIIC. *Cells*. 2024;13(10):877. doi:10.3390/cells13100877.

53. Marcó S, Pujol A, Roca C, Motas S, Ribera A, Garcia M, Molas M, Villacampa P, Melia CS, Sánchez V, Sánchez X, et al. Progressive neurologic and somatic disease in a novel model of human mucopolysaccharidosis type IIIC. *Dis Model Mech*. 2016;9:999–1013. doi:10.1242/dmm.025171.

54. Lau AA, Crawley AC, Hopwood JJ, Hemsley KM. Open field locomotor activity and anxiety-related behaviors in mucopolysaccharidosis type IIIA mice. *Behav Brain Res*. 2008;191(1):130–36. doi:10.1016/j.bbr.2008.03.024.

55. Gao C, Jiang J, Tan Y, Chen S. Microglia in neurodegenerative diseases: mechanism and potential therapeutic targets. *Sig Transduct Target Ther*. 2023;8(1):359. doi:10.1038/s41392-023-01588-0.

56. Xu Y, Gao W, Sun Y, Wu M. New insight on microglia activation in neurodegenerative diseases and therapeutics. *Front Neurosci*. 2023;17:1308345. doi:10.3389/fnins.2023.1308345.

57. Lull ME, Block ML. Microglial activation and chronic neurodegeneration. *Neurotherapeutics*. 2010;7(4):354–65. doi:10.1016/j.nurt.2010.05.014.

58. Wilkinson FL, Holley RJ, Langford-Smith KJ, Badrinath S, Liao A, Langford-Smith A, Cooper JD, Jones SA, Wraith JE, Wynn RF, Merry CLR, et al. Neuropathology in mouse models of mucopolysaccharidosis type I, IIIA and IIIB. Kremer EJ, ed. *PLoS ONE*. 2012;7(4):e35787. doi:10.1371/journal.pone.0035787.

59. Willing AE, Garbuzova-Davis SN, Zayko O, Derasari HM, Rawls AE, James CR, Mervis RF, Sanberg CD, Kuzmin-Nichols N, Sanberg PR. Repeated administrations of human umbilical cord blood cells improve disease outcomes in a mouse model of Sanfilippo syndrome type III B. *Cell Transplant*. 2014;23(12):1613–30. doi:10.3727/096368914X676916.

60. Ohmi K, Greenberg DS, Rajavel KS, Ryazantsev S, Li HH, Neufeld EF. Activated microglia in cortex of mouse models of mucopolysaccharidoses I and IIIB. *Proc Natl Acad Sci USA*. 2003;100(4):1902–907. doi:10.1073/pnas.252784899.

61. Taherzadeh M, Zhang E, Londono I, De Leener B, Wang S, Cooper JD, Kennedy TE, Morales CR, Chen Z, Lodygensky GA, Pshezhetsky AV. Severe central nervous system demyelination in Sanfilippo disease. *Front Mol Neurosci*. 2023;16:1323449. doi:10.3389/fnmol.2023.1323449.

62. Papageorgiou IE, Lewen A, Galow LV, Cesetti T, Scheffel J, Regen T, Hanisch UK, Kann O. TLR4-activated microglia require IFN-γ to induce severe neuronal dysfunction and death in situ. *Proc Natl Acad Sci USA*. 2016;113(1):212–17. doi:10.1073/pnas.1513853113.

63. Holley RJ, Ellison SM, Fil D, O'Leary C, McDermott J, Senthivel N, Langford-Smith AWW, Wilkinson FL, D'Souza Z, Parker H, Liao A, et al. Macrophage enzyme and reduced inflammation drive brain correction of mucopolysaccharidosis IIIB by stem cell gene therapy. *Brain*. 2018;141(1):99–116. doi:10.1093/brain/awx311.

64. Nagel L, Oliveira R, Pshezhetsky AV, Morales CR. HGSNAT enzyme deficiency results in accumulation of heparan sulfate in podocytes and basement membranes. *Histol Histopathol*. 2019;34(12):1377–85. doi:10.14670/HH-18-131.

65. Yeagy BA, Harrison F, Gubler MC, Koziol JA, Salomon DR, Cherqui S. Kidney preservation by bone marrow cell transplantation in hereditary nephropathy. *Kidney Int*. 2011;79(11):1198–206. doi:10.1038/ki.2010.537.

66. Lau AA, Shamsani NJ, Winner LK, Hassiotis S, King BM, Hopwood JJ, Hemsley KM. Neonatal bone marrow transplantation in MPS IIIA mice. *JIMD Rep*. 2012;8:121–32. doi:10.1007/8904_2012_169.

67. Sergijenko A, Langford-Smith A, Liao AY, Pickford CE, McDermott J, Nowinski G, Langford-Smith KJ, Merry CL, Jones SA, Wraith JE, Wynn RF, et al. Myeloid/microglial driven autologous hematopoietic stem cell gene therapy corrects a neuronopathic lysosomal disease. *Mol Ther*. 2013;21(10):1938–49. doi:10.1038/mt.2013.141.